RADAR SCATTERING IN FIRN AND ITS IMPLICATIONS FOR VHF/UHF ORBITAL ICE SOUNDING

Riley Culberg¹, Dustin M. Schroeder^{1,2}

¹ Department of Electrical Engineering, Stanford University ² Department of Geophysics, Stanford University

ABSTRACT

Radar sounding of ice from orbit has been successful on Mars [1], is planned for the Galilean satellites [2], and is attractive for earth [3] as a complement to current airborne instruments [4], but of major concern is the poorly constrained but potentially seriously limiting contribution of firn clutter [5]. To inform this issue, we analytically model electromagnetic scattering in the upper 100 meters of the ice column for continental ice sheets and evaluate the effects of variable platform altitude, frequency, and range resolution on clutter power. Our results show that volume scattering from air inclusions is insignificant and unlikely to constrain deep ice sounding. Rather, firn scattering is dominated by quasispecular reflections from layers of varying density which, at orbital altitudes, may contribute significantly to clutter due to the small angles of illumination. This layer clutter can be mitigated by a careful choice of range resolution for center frequencies below 200 MHz, but is practically unavoidable above 250 MHz. Firn layer clutter is likely to significantly constrain UHF orbital ice sounding, making a VHF instrument the more practical choice.

Index Terms— ice penetrating radar, orbital sounding, clutter, firn

1. INTRODUCTION

Airborne radar sounding is one of only a few remote sensing techniques for studying conditions in and under the continental ice sheets [6]. A satellite sounding instrument would significantly improve the spatial and temporal coverage of these observations. The most widely used airborne radar sounding systems operate between 60 and 200 MHz [4], but orbital feasibility studies have also considered instrument center frequencies at 435 MHz [7] and 45 MHz [8]. Therefore, it is important to understand the trade-offs in system capability that come with these design choices.

In particular, although UHF orbital sounding is attractive for a number of practical reasons, results from the European Space Agency's airborne testbed, POLARIS, suggest that a more thorough assessment of its feasibility is needed. Most data collected by POLARIS show strong returns in the top 100m meters of the ice sheet which are rarely observed in

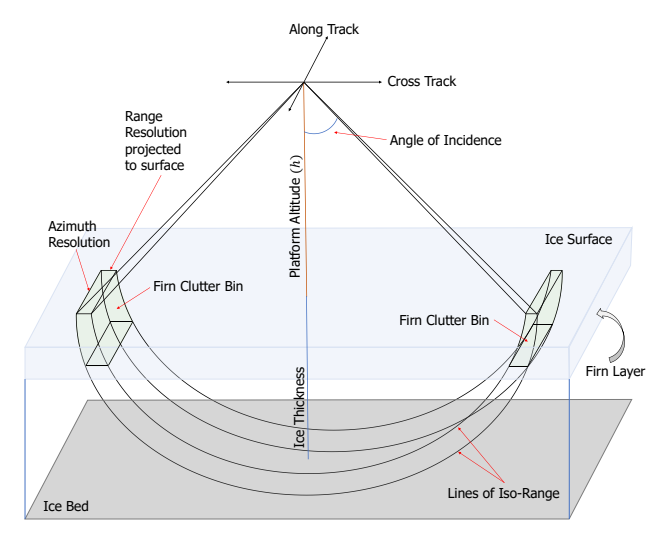


Fig. 1. Radar sounding geometry.

VHF data [9]. A similar signature in data collected by the University of Kansas's Center for the Remote Sensing of Ice and Snow (CReSIS) Accumulation Radar [10], which operates at 725 MHz, suggests that the phenomenon may be particular to UHF systems.

Dall, et al [5] used an empirical model derived from the POLARIS data to show that in an orbital sounding configuration, clutter from these near-surface scatterers could mask the bed return over much of Antarctica. However, empirical models are not well suited to investigating how choices of instrument parameters might mitigate this effect. To inform these decisions, we develop and apply two glaciologically-informed analytic models for electromagnetic scattering in firn, validate them against the existing airborne radar data, and discuss the implications of each model for orbital sounding instrument design.

2. FIRN MODELS

2.1. Random Particle Scattering Model

In this model, we treat firn as a porous ice layer filled with air bubbles, parametrized by a depth-averaged pore radius and a depth-porosity profile.

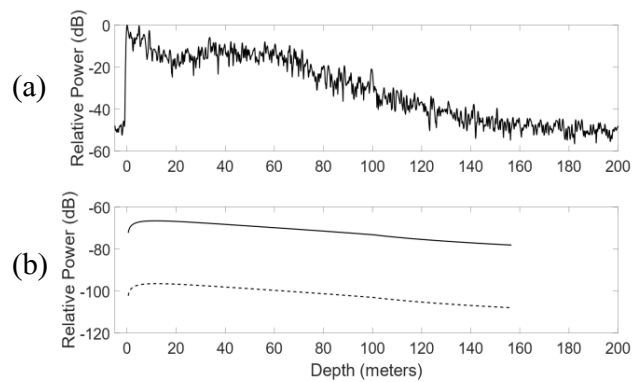


Fig. 2. Qualitative comparison of Accumulation Radar power trace (a) and modeled power traces due to volume scattering (b). In (a), the surface reflection has been normalized to 0 dB. In (b), power is normalized to a specular reflection at the air-firn interface.

The approximate volume scattering radar equation derived from [11] relates the radar system parameters and properties of the illuminated ice volume to the power received by the radar.

$$P_{R} = \frac{P_{T}G^{2}\lambda^{2}}{(4\pi)^{3}n_{ice}^{2}}\sigma^{0} \int_{0}^{d} \left(\frac{3\phi(z)}{4\pi r^{3}}\right) V(z) \left(\frac{1}{R(z)^{4}}\right) e^{-2\tau z} dz \qquad (1)$$

 P_R = received power P_T = transmitted power G = antenna gain λ = free-space wavelength $\phi(z)$ = porosity γ = average pore radius γ = range to radar γ = index of refraction of ice γ = firn layer depth γ = extinction coefficient of a single pore γ = extinction coefficient of a single pore

Figure 1 shows the sounding geometry for synthetic aperture (SAR) focused sounder data. The illuminated volume is estimated from an ellipsoidal fit to the lines of isorange. We use an open source Mie solver [12] to calculate the backscatter and extinction coefficients for spherical air-filled pores ($\epsilon_r = 1$) in glacial ice ($\epsilon_r = 3.15$). As this model treats scattering as the result of independent, spherical, and randomly distributed air inclusions in ice, the angular scattering pattern is isotropic and the model will tend to overestimate the scattered power.

We apply this model to simulate the depth-power profile at the B26 site of the 1995 North Greenland Traverse and compare with an adjacent radar trace collected by the Accumulation Radar [13]. The depth-porosity profile is derived from a third order polynomial fit to the depth-density profile of the ice core [14], which is converted to porosity by (2) where the density of ice is 917 kg/m³.

$$\phi(z) = 1 - \frac{\rho(z)}{\rho_{ice}} \tag{2}$$

We consider a range of physically plausible pore sizes from 1mm to 1cm in diameter [15] and use the system parameters of the Accumulation Radar.

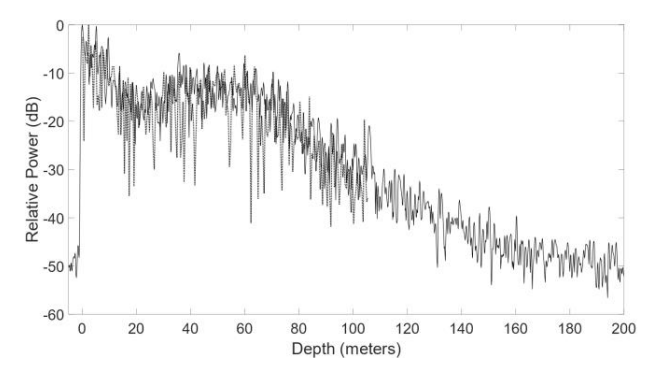


Fig. 3. Comparison of radar trace from the Accumulation Radar (solid line) and a simulated radar trace (dotted line) using high resolution density profiles from the B26 ice core. The surface reflection has been normalized to 0 dB.

This model fails to reproduce either the magnitude or relative trend in near-surface power observed in the Accumulation Radar trace for any set of physically reasonable parameters. Even considering water-filled pore space [16], modeled volume scattering power is always well below the observed firn returns due to the simultaneous increase in attenuation.

Increased volume scattering with increased frequency cannot adequately explain the anomalous strong firn returns in UHF radar data.

2.2. Quasi-Specular Layer Reflection Model

Lewis, et al [10] proposed that strong firn returns are the result of quasi-specular reflections from layers of varying density. They show that the standard deviation of firn density in the B26 ice core matches well with the near-surface power trend in an adjacent Accumulation Radar trace. Following this hypothesis, we model firn as a layered medium where the permittivity of each layer is calculated from the local density following the empirical relationship in (3) given by [17]. The depth of each layer is given by the sampling frequency of the empirical density data set.

$$\epsilon_r = \left(1 + 0.845\rho(z)\right)^2 \tag{3}$$

We assume that for a pulsed, linear frequency modulated waveform, the only part of this layered system which is both simultaneously illuminated and where interference effects are significant is a stack of layers of depth equal to the range resolution. Therefore, we estimate the effective reflection coefficient of each range bin by using the transfer matrix method to solve for total reflectance from this multilayer dielectric structure [18], where the half space above the range bin has density equal to the last layer above the stack and the half space below the range bin has density equal to the first layer below the stack.

We apply this model to high resolution density measurements taken every 1 mm over the top 119 meters of the B26 ice core [14]. We simulate the reflection coefficient of each range bin for a radar system with a center frequency of 725 MHz and 320 MHz of bandwidth to match the Accumulation Radar. Comparing our simulated trace to the

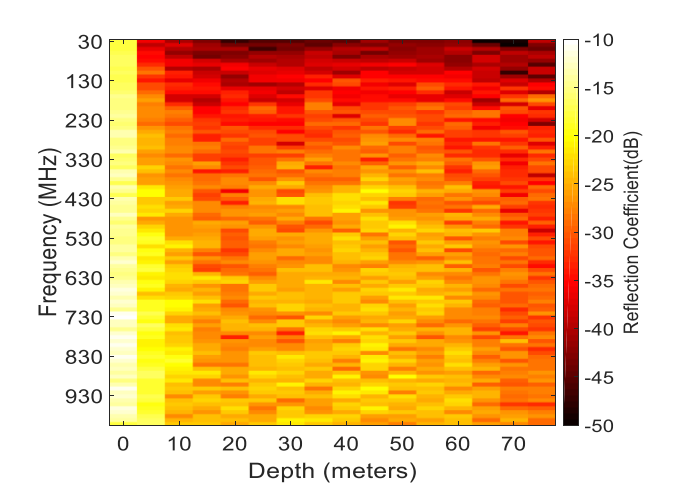


Fig. 4. Modeled layer reflection coefficients as a function of depth for a range of center frequencies and a fixed range resolution of 5 meters.

radar trace nearest the core site [13], we see excellent agreement in both the magnitude and relative trend of the power between the observed and modeled data (see Figure 3).

The dominant scattering mechanism in firn is likely thin film interference of quasi-specular reflections from multiple, simultaneously illuminated layers of varying density.

3. ORBITAL SOUNDING IMPLICATIONS

3.1. Random Particle Scattering Model

Although this scattering mechanism is negligible in airborne configurations, it is still valuable to consider whether it might become a concern for orbital sounding. An increase in platform altitude or decrease in range resolution will increase the illuminated ice volume, resulting in greater volume clutter power. We evaluate firn volume clutter for the parameters given in Table I.

TABLE I.

Parameter	Range
Altitude	100-300 km
Center Frequency	30-500 MHz
Range Resolution	0.5-20 m
Pore Diameter	1mm – 1cm
Pore Saturation	0 - 100%

Although there is significant variation in clutter power within this parameter space, we find no combination where volume clutter is the limiting factor in the detecting the bed in SAR focused sounder data. The signal-to-noise ratio or attenuation generally becomes a limiting factor first. Therefore, volume clutter from particle scattering does not significantly constrain system design choices. This finding is consistent with previous work assessing the impact of volume scattering on radar sounding of Europa [19].

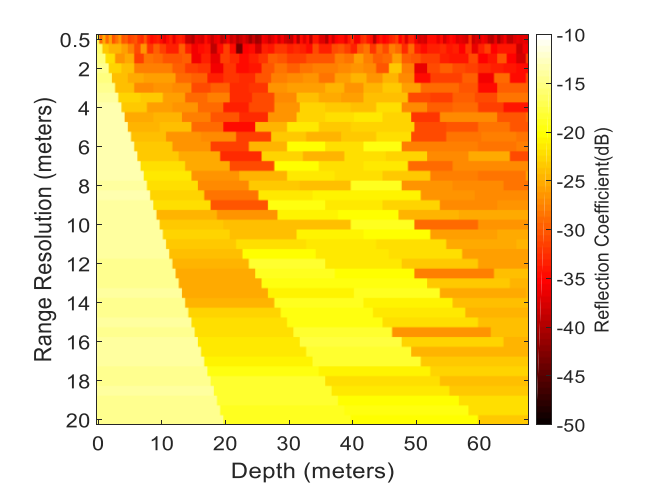


Fig. 5. Modeled layer reflection coefficients as a function of depth for various range resolutions and a fixed frequency of 435 MHz.

3.2. Quasi-Specular Layer Reflection Model

Specular reflectors are typically not considered a source of clutter for monostatic radars since they reflect power back to the radar only at normal incidence [20]. However, even small levels of surface roughness, coupled with a finite illumination area, can produce appreciable backscatter at small angles of incidence [21]. This angular scattering pattern is well approximated by a Gaussian function where backscattered power decreases rapidly as the angle of incidence increases [21]. In airborne systems, clutter bins which map to the bed are illuminated at very large incidence angles, equating to relatively low power. At orbital altitudes, especially after accounting for refractive focusing in ice, the angle of incidence is significantly smaller. At 300 km altitude, clutter bins which map to 1000 meters depth will be illuminated at an angle of only 6 degrees off-nadir. Dall, et al [5] reports that, given empirical angular scattering patterns derived from POLARIS data, the resulting firn layer clutter obscures the bed in two-thirds of their simulated scenarios.

Although the angular scattering pattern of firn is poorly constrained, relative nadir power is a reasonable proxy for relative clutter power. Therefore, we investigate the change in both the magnitude and depths of the strong reflection coefficients as a function of center frequency and range resolution.

We use six high-resolution ice core density profiles – three from Antarctic and three from Greenland [14], [22]–[25] to model range bin reflection coefficients for frequencies from 30-1000 MHz and range resolutions from 0.5-20 meters. We then average the depth-reflection coefficient profiles over the six density models. In general, decreasing center frequency and increasing range resolution lowers both the average reflection coefficient magnitude and the range of depths over which high coefficients are observed. Figures 4 and 5 show examples of the trends for fixed resolution and fixed frequency respectively.

Our analysis suggests that for frequencies below 80 MHz, density layer power is relatively insensitive to range resolution. From 80-200 MHz, layer power can be limited to an average of 25 dB below the surface reflection with range resolutions corresponding to fractional system bandwidths of less than 50%. Between roughly 250 MHz and 3 GHz, this mitigation is not possible, requiring fractional bandwidths in excess of 100%.

4. CONCLUSIONS

Radar scattering in firn is best modeled as quasi-specular reflection from multiple, simultaneously illuminated layers of variable density. Volume scattering from air inclusions is negligible by comparison.

We find that even at orbital altitudes, volume clutter is insufficient to constrain deep ice sounding so long as alongtrack SAR focusing is employed. However, clutter from quasi-specular firn layers is a significant concern for platform altitudes above approximately 30 km. For systems operating at or below 200 MHz, this effect can be mitigated by a careful choice of range resolution. This mitigation is not possible for UHF sounders as the fractional bandwidths required to achieve the necessary range resolutions would be in excess of 100%. Constraining the angular scattering behavior of firm density layers will be critical in formally bounding both the altitudes and layer power levels of concern and could potentially permit some relaxation of these frequency bounds. Regardless, firn layer clutter is likely to significantly constrain UHF orbital ice sounding, making a VHF instrument the more practical choice at this time.

5. ACKNOWLEDGEMENTS

We acknowledge the use of data from CReSIS generated with support from the University of Kansas, NASA Operation IceBridge grant NNX16AH54G, NSF grant ACI-1443054, Lilly Endowment Incorporated, and Indiana METACyt Initiative.

6. REFERENCES

- [1] J. J. Plaut *et al.*, "Subsurface radar sounding of the south polar layered deposits of Mars," *Science*, vol. 316, no. 5821, pp. 92–95, 2007.
- [2] L. Bruzzone, G. Alberti, C. Catallo, A. Ferro, W. Kofman, and R. Orosei, "Subsurface radar sounding of the jovian moon ganymede," *Proc. IEEE*, vol. 99, no. 5, pp. 837–857, 2011.
- [3] F. Hélière, C. Lin, H. Corr, and D. Vaughan, "Radio Echo Sounding of Pine Island Glacier, West Antarctica: Aperture Synthesis Processing and Analysis of Feasibility From Space," *IEEE Trans. Geosci. Remote Sens.*, vol. 45, no. 8, pp. 2573–2582, 2007.
- [4] C. Leuschen *et al.*, "Development of a Multi-Frequency Airborne Radar Instrumentation Package for Ice Sheet Mapping and Imaging," in *IEEE MTT-S International Microwave Symposium*, 2010
- [5] J. Dall, H. F. J. Corr, N. Walker, B. Rommen, and C. Lin,

- "Sounding the Antarctic ice sheet from space: a feasibility study based on airborne P-band radar data," *IGARSS 2018*, pp. 4142–4145, 2018.
- [6] J. A. Dowdeswell and S. Evans, "Investigations of the form and flow of ice sheets and glaciers using radio-echo sounding," *Reports Prog. Phys.*, vol. 67, no. 10, pp. 1821–1861, 2004.
- [7] J. Dall *et al.*, "ESA'S POLarimetric Airborne Radar Ice Sounder (POLARIS): design and first results," *IET Radar, Sonar Navig.*, vol. 4, no. 3, p. 488, 2010.
- [8] A. Freeman, X. Pi, and E. Heggy, "Radar Sounding Through the Earth's Ionosphere at 45 MHz," *IEEE Trans. Geosci. Remote Sens.*, vol. 55, no. 10, pp. 5833–5842, 2017.
- [9] J. Dall, "A backscattering and propagation model for radar sounding of ice sheets," *Int. Geosci. Remote Sens. Symp.*, vol. 2016–Novem, no. 3, pp. 7088–7091, 2016.
- [10] C. Lewis *et al.*, "Airborne fine-resolution UHF radar: An approach to the study of englacial reflections, firn compaction and ice attenuation rates," *J. Glaciol.*, vol. 61, no. 225, pp. 89–100, 2015.
- [11] F. T. Ulaby and D. G. Long, *Microwave Radar and Radiometric Remote Sensing*. Ann Arbor, MI: The University of Michigan Press, 2014.
- [12] C. Mätzler, "MATLAB Mie Solver v2." 2002, https://scattport.org/index.php/programs-menu/mie-type-codes-menu/111-mie-matlab-maetzler.
- [13] CReSIS, "Accumulation Radar Data." Lawrence, Kansas, USA, 2011, http://data.cresis.ku.edu/.
- [14] H. Miller and M. Schwager, "Density of ice core ngt37C95.2 from the North Greenland Traverse." PANGEA, 2000, https://doi.org/10.1594/PANGAEA.57798.
- [15] K. Langley *et al.*, "Use of C-band ground penetrating radar to determine backscatter sources within glaciers," *IEEE Trans. Geosci. Remote Sens.*, vol. 45, no. 5, pp. 1236–1245, 2007.
- [16] A. K. Kendrick *et al.*, "Surface Meltwater Impounded by Seasonal Englacial Storage in West Greenland," *Geophys. Res. Lett.*, pp. 1–8, 2018.
- [17] A. Kovacs, A. J. Gow, and R. M. Morey, "A reassessment of the in-situ dielectric constant of polar firn," no. CRREL-93-26, p. 29, 1993.
- [18] P. Yeh, Optical Waves in Layered Media. Hoboken, NJ: Wiley, 2005
- [19] Y. Aglyamov, D. M. Schroeder, and S. D. Vance, "Bright prospects for radar detection of Europa's ocean," *Icarus*, vol. 281, pp. 334–337, 2017.
- [20] F. T. Ulaby, R. K. Moore, and A. K. Fung, *Microwave Remote Sensing: Active and Passive, Volume II.* Reading, Massachusets: Addison-Wesley Publishing Company, 1982.
- [21] S. K. Nayar, K. Ikeuchi, and T. Kanade, "Surface Reflection: Physical and Geometrical Perspectives," *IEEE Trans. Pattern Anal. Mach. Intell.*, vol. 13, no. 7, pp. 611–634, 1991.
- [22] H. Miller and M. Schwager, "Density of ice core ngt42C95.2 from the North Greenland Traverse." PANGEA, 2000, https://doi.pangaea.de/10.1594/PANGAEA.57655.
- [23] H. Oerter *et al.*, "Physical properties and accumulation rates in Dronning Maud Land, Antarctica." PANGEA, 2000, https://doi.org/10.1594/PANGAEA.728162.
- [24] S. Gerland and F. Wilhelms, "Continuous density log of icecore BER11C95_25." PANGEA, 1999, https://doi.org/10.1594/PANGAEA.227732.
- [25] F. Wilhelms, "Density of ice core ngt27C94.2 from the North Greenland Traverse." PANGEA, 2000, https://doi.org/10.1594/PANGAEA.57296.